CHEMISTRY AND TECHNOLOGY OF INORGANIC MATERIALS

ХИМИЯ И ТЕХНОЛОГИЯ НЕОРГАНИЧЕСКИХ МАТЕРИАЛОВ

ISSN 2686-7575 (Online)

https://doi.org/10.32362/2410-6593-2022-17-5-439-449

UDC 666.3.015.4

RESEARCH ARTICLE

Effect of activating additives on the cold sintering process of $(MnFeCoNiCu)_3O_4$ high-entropy ceramics

Andrey V. Smirnov[1,✉], Yuri D. Ivakin[1,2], Maxim V. Kornyushin[1], Anastasia A. Kholodkova[1,2], Alexander A. Vasin[1], Sofia Ayudinyan[3], Hasmik V. Kirakosyan[3]

[1]Mobile Solutions Engineering Center, MIREA – Russian Technological University, Moscow, 119454 Russia
[2]Faculty of Chemistry, M.V. Lomonosov Moscow State University, Moscow, 119991 Russia
[3]A.B. Nalbandyan Institute of Chemical Physics, National Academy of Sciences, Yerevan, 0014 Armenia
[✉]Corresponding author, e-mail: smirnov_av@mirea.ru

Abstract

Objectives. *To obtain experimental data on the effect of activating additive type on the cold sintering process of $(MnFeCoNiCu)_3O_4$ high-entropy ceramic. The following substances were used as activating additives: ammonium acetate (CH_3COONH_4), acetic acid (CH_3COOH), ammonium chloride (NH_4Cl), potassium fluoride dihydrate ($KF{\cdot}2H_2O$), lithium fluoride (LiF), sodium fluoride (NaF), and sodium hydroxide (NaOH).*

Methods. *Synthesis of the initial powder by low-temperature self-propagating method; investigation of the powder particles size distribution by laser diffraction method; analysis of the particle shape and compacted sample microstructure by scanning electron microscopy; investigation of the phase composition by X-ray phase analysis; high-entropy ceramic sample consolidation by cold sintering process. The density of the initial powder and the relative density of cold sintered samples were determined by the Archimedes method.*

Results. *Samples with a relative density of over 0.70 were obtained using distilled water, CH_3COONH_4 and NaOH during cold sintering at 300°C, with a holding time of 30 min and pressure 315 MPa.*

Conclusions. *For the first time, the effect of the type of activating additive on the relative density of high-entropy ceramics $(MnFeCoNiCu)_3O_4$ samples obtained by cold sintering process has been experimentally demonstrated. The samples microstructures have pronounced differences: 20 wt % distilled water does not lead to grain growth, with only their compaction to 0.71 relative density observed; however, the addition of 0.1 wt % CH_3COONH_4 and NaOH increases the average grain size when reaching similar relative densities (0.70 and 0.71, respectively). X-ray diffraction analysis showed that the cold sintering process does not lead to a change in the phase composition of the initial $(MnFeCoNiCu)_3O_4$ powder, confirming the preservation of the high-entropy structure.*

Keywords: *high-entropy ceramics, oxide ceramics, cold sintering process, sintering, phase composition*

For citation: Smirnov A.V., Ivakin Yu.D., Kornyushin M.V., Kholodkova A.A., Vasin A.A., Ayudinyan S., Kirakosyan H.V. Effect of activating additives on the cold sintering process of $(MnFeCoNiCu)_3O_4$ high-entropy ceramics. *Tonk. Khim. Tekhnol. = Fine Chem. Technol.* 2022;17(5):439–449 (Russ., Eng.). https://doi.org/10.32362/2410-6593-2022-17-5-439-449

НАУЧНАЯ СТАТЬЯ

Влияние активирующих добавок на процесс холодного спекания высокоэнтропийной керамики $(MnFeCoNiCu)_3O_4$

А.В. Смирнов[1,✉], Ю.Д. Ивакин[1,2], М.В. Корнюшин[1], А.А. Холодкова[1,2], А.А. Васин[1], С. Аюдинян[3], А.В. Киракосян[3]

[1]Инжиниринговый центр мобильных решений, МИРЭА – Российский технологический университет, Москва, 119454 Россия
[2]Химический факультет, Московский государственный университет им. М.В. Ломоносова, Москва, 119234 Россия
[3]Институт химической физики им. А.Б. Налбандяна, Ереван, 0014 Армения
[✉]Автор для переписки, e-mail: smirnov_av@mirea.ru

Аннотация

Цели. *Получение экспериментальных данных о влиянии вида активирующей добавки на процесс холодного спекания высокоэнтропийной керамики состава $(MnFeCoNiCu)_3O_4$. В качестве активирующих добавок были использованы: ацетат аммония (CH_3COONH_4), уксусная кислота (CH_3COOH), аммоний хлористый (NH_4Cl), калий фтористый 2-х водный $(KF{\cdot}2H_2O)$, литий фтористый (LiF), натрий фтористый (NaF), гидроксид натрия (NaOH).*
Методы. *Синтез исходного порошка методом низкотемпературного самораспространяющегося синтеза; исследование гранулометрического состава порошка методом лазерной дифракции; анализ формы частиц и микроструктуры скомпактированных образцов методом сканирующей электронной микроскопии; анализ фазового состава методом рентгенофазового анализа; консолидация образцов высокоэнтропийной керамики методом холодного спекания; плотность исходного порошка и относительная плотность образцов керамики холодного спекания определялись методом Архимеда.*
Результаты. *Образцы с относительной плотностью свыше 0.70 получены с применением дистиллированной воды, CH_3COONH_4 и NaOH в процессе холодного спекания при температуре 300°C, времени выдержки 30 мин и давлении прессования 315 МПа.*

Выводы. *Впервые экспериментально показано влияние вида активирующей добавки на относительную плотность образцов высокоэнтропийной керамики $(MnFeCoNiCu)_3O_4$, полученных с помощью процесса холодного спекания. Микроструктуры образцов имеют выраженные отличия: 20 мас. % дистиллированной воды не приводит к росту зерен, наблюдается только их уплотнение до 0.71 относительной плотности; при добавлении 0.1 мас. % CH_3COONH_4 и NaOH наблюдается рост среднего размера зерен при достижении близких показателей относительной плотности (0.70 и 0.71 соответственно). Рентгенодифракционный анализ показал, что процесс холодного спекания порошка $(MnFeCoNiCu)_3O_4$ не приводит к изменению фазового состава исходного порошка, что свидетельствует о сохранении высокоэнтропийной структуры.*

Ключевые слова: *высокоэнтропийная керамика, оксидная керамика, процесс холодного спекания, спекание, фазовый состав*

Для цитирования: Смирнов А.В., Ивакин Ю.Д., Корнюшин М.В., Холодкова А.А., Васин А.А., Аюдинян С., Киракосян А.В. Влияние активирующих добавок на процесс холодного спекания высокоэнтропийной керамики $(MnFeCoNiCu)_3O_4$. *Тонкие химические технологии*. 2022;17(5):439–449. https://doi.org/10.32362/2410-6593-2022-17-5-439-449

INTRODUCTION

High-entropy materials were first described in 2004 as innovative metallic disordered multicomponent alloys having promising applications [1]. The number of combinations of composition components that can be covered using this approach is almost limitless, and so far a very limited number of options have been explored. However, several high-entropy alloys have previously been shown to have exceptional mechanical and performance properties that are superior to conventional alloys [2]. Later, in 2015, entropy stabilization in a mixture of oxides was demonstrated, and the first samples of the so-called high-entropy ceramics were obtained. It has been shown that high-entropy ceramic systems have promising properties for a wide range of applications: thermal barrier coatings, thermoelectrics, catalysts, batteries, and wear-resistant coatings [3]. In recent years, several high-entropy oxide systems have been studied, such as ferrimagnetic $(CoCrFeMnNi)_3O_4$ [4, 5] and ferromagnetic $(CoCrFeMnZn)_3O_4$ and $(CoCrFeNiZn)_3O_4$ [6]; perovskites with rare earth elements ($La(CoCrFeMnNi)O_3$), which exhibit a complex magnetic state with a predominance of antiferromagnetic interactions [7]. It has been found that a high-entropy oxide ceramic material with a rock-salt type structure (MgCoNiCuZn)O exhibits long-range magnetic order despite the structural disorder of randomly distributed magnetic ions. It is assumed that similar magnetic properties can be realized in high-entropy oxide ceramic materials with different types of crystal lattice and different compositions of elements, in particular, in the $(MnFeCoNiCu)_3O_4$ system [8].

When studying the properties of the above-described promising high-entropy oxide ceramic materials, one of the main arising problems is how to preserve the high-entropy structure of the initial powder materials during their sintering. High sintering temperatures (usually more than 1000°C) lead to disruption of the high-entropy structure as a result of the phase transformations, evaporation and chemical reactions, as well as the decomposition of high-entropy phases [3]. For stable production of high-entropy ceramic samples, it is necessary to use consolidation methods at temperatures not exceeding the synthesis temperature of initial high-entropy ceramic powders, which are within the range of 350–750°C [3, 9].

The cold sintering process (CSP), an innovative ceramic sintering method that uses a liquid phase, compression-molding pressure and temperatures below 550°C, is under active study and development [10, 11]. It has been found that the participation in CSP of a liquid phase (most often water or aqueous solutions of acids and alkalis) can significantly reduce the sintering temperatures of oxide ceramic materials down to the range of 200–400°C and lower, in some cases even to room temperature [12]. In addition, some materials, such as ZnO, can be compacted to more than 90% of their theoretical density in less than 15 min at temperatures below 300°C [13]. The scheme of the CSP is shown in Fig. 1.

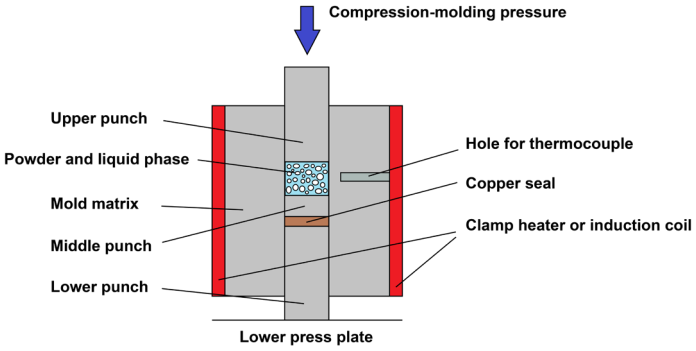

Fig. 1. Scheme of the cold sintering process.

The main CSP parameters are: pressing force; temperature in the mold; time of exposure under the action of a given pressure and temperature; activating additive type and concentration; liquid phase concentration; ceramic powder material properties (its solubility, particle size and granulometric composition (Fig. 2) [14]. These parameters are selected for each specific material experimentally. The mechanism or mechanisms of the CSP are under study. To date, three mechanisms of mass transfer in the CSP are proposed in the literature: dissolution–precipitation [11]; mass transfer due to surface diffusion in a layer with a high content of defects formed as a result of dissociative adsorption of water by oxide particles [13]; mass transfer due to surface spreading and coalescence of particles owing to the appearance of solid-phase mobility of the oxide structure as a result of the exchange of water molecules between the medium and the forms of water bound in the structure of oxide particles [15].

The choice of additives for CSP activation is based on theories concerning the process mechanism. These can be additives that increase the oxide particles solubility in an aqueous medium due to a change in pH. The addition of NaOH increases the aqueous solution pH, creating an alkaline environment. Acetic acid reduces the solution pH and promotes the dissolution of oxides in the acidic environment. When adsorbed on oxide particles, the acid proton increases the content of hydroxyl groups (bound forms of water in the structure of oxides) in them to increase structural mobility [16]. Ammonium acetate or ammonium chloride added to water also create an acidic environment due to hydrolysis when the temperature rises. In addition, studies on CSP have shown that the acetate ion is able to diffuse into the volume of oxide particles and exchange with the medium thus causing an increase in structural mobility [16, 17]. The addition of fluorides during hydrolysis leads to the formation of HF, which can increase the solubility of oxides also due to the formation of fluoride complexes [18]. Currently, there is an absence in the CSP literature of works about the effect of activating additives on the composition $(MnFeCoNiCu)_3O_4$, as well as a lack of works on high-entropy ceramics in general.

In [19], the fundamental possibility of obtaining samples of high-entropy ceramics $(MnFeCoNiCu)_3O_4$ by CSP using 20 wt % of distilled water as a liquid phase was experimentally shown for the first time. Ceramic samples with a porosity of 28–31% were obtained at 300°C, holding times of 3, 30, and 60 min and a compression-molding pressure of 315 MPa.

The purpose of this study is to obtain new experimental data on the effect of the activating additive type on the CSP of high-entropy ceramics $(MnFeCoNiCu)_3O_4$. The influence of the activating additive type was evaluated by the samples relative density. The densest samples were subjected to analysis of the microstructure and phase composition.

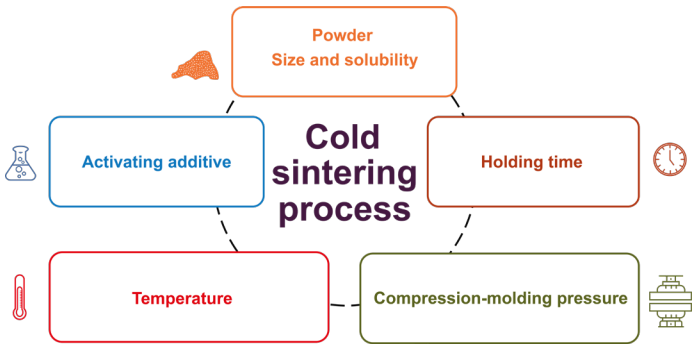

Fig. 2. Main parameters of the cold sintering process [14].

MATERIALS AND METHODS

The powder of high-entropy oxide ceramic material $(MnFeCoNiCu)_3O_4$ synthesized by low-temperature self-propagating synthesis (or bulk combustion) in air from an equimolar mixture of Mn, Fe, Co, Ni, and Cu metal nitrates was used as a starting material. To prepare a mixture of precursors, metal nitrate hydrates $(Me(NO_3)_n)$ (*Sigma-Aldrich*, USA) were dissolved together with organic fuel (citric acid) in own-made deionized water to obtain a saturated solution. The homogeneous mixture was poured into a quartz glass beaker and heated on an electric heater. After the evaporation of water, a viscous liquid (sol, then gel) was formed, which spontaneously

ignited at a temperature above 200°C (so-called bulk combustion accompanied by gas evolution and smoke). To monitor the reaction in various thermal conditions, we used measurements with a chromel-alumel thermocouple (*NPP "Etalon,"* Russia). The maximum synthesis temperature was about 450°C. After cooling, the synthesis product was removed from the beaker and ground in an agate mortar.

The CSP was carried out in a steel mold with induction heating (Fig. 3a). The mold assembly contained three punches: upper, middle and lower (11 mm in diameter). A mixture of $(MnFeCoNiCu)_3O_4$ powder with a liquid phase was located between the upper and middle punches, while a copper sealing ring was placed between the middle and lower punches (Fig. 3b). The seal was used to prevent the mixture from being squeezed out of the gaps in the mold during compression 0.4 g of $(MnFeCoNiCu)_3O_4$ powder and 0.08 mL of water (20 wt %) were mixed in a bowl under thorough stirring immediately before placing into the mold. The thermocouple was fixed in the mold in a cavity next to the sample. The mold with the induction heater was installed along the hydraulic press axis. The powder shrinkage in the mold was controlled by measuring the axial displacement of the hydraulic press lower platform by using a mechanical dial indicator (with a division value of 10 μm) (*VladPromash*, Russia) mounted on the hydraulic press frame.

The following modes of the cold baking process were used: baking temperature—250 and 300°C, time of heating to baking temperature—20 min, and holding time—30 min. The modes were chosen on the basis of the results of [19]. In all the experiments, the amount of the liquid phase was 20 wt %: distilled water or an aqueous solution of 0.1 wt % of an activating additive. The following substances were used as activating additives: ammonium acetate (CH_3COONH_4) (*Khimprom-M*, Russia), acetic acid (CH_3COOH) (*RKhZ "NORDIKS,"* Russia), ammonium chloride (NH_4Cl) (*Khimprom-M*, Russia), potassium fluoride dihydrate ($KF{\cdot}2H_2O$) (*RKhZ "Nordiks,"* Russia), lithium fluoride (LiF) (*Alfa Aesar*, USA), sodium fluoride (NaF) (*Alfa Aesar*, USA), and sodium hydroxide (NaOH) (*Alfa Aesar*, USA). All the reagents were of purissimum or analytical quality.

Characterization of the initial powder by particle size distribution was carried out using a laser particle size analyzer LS 13 320 MW (*Beckman Coulter*, USA). Before measuring the granulometric composition, the initial powder sample was deagglomerated by placing it in a glass tube with water and subjecting it to ultrasound in an ultrasonic bath at a power of 60 W. The density of the initial powder and the relative density of samples of cold-sintered ceramics were estimated according to the Archimedes method. The morphology of the initial powder and the microstructure of the ceramic samples were studied by scanning electron microscopy (SEM) using a JSM-6390 LA microscope (*JEO*, Tokyo, Japan). The average grain size of the ceramic samples was determined by the analysis of SEM images of the samples fractures. The diameter of samples with a distinct contour was measured. In the end, the results of the measurements contain both the sizes of rare particles and the sizes of their dense aggregates. Phase analysis of the synthesized powder and ground ceramic samples

(a) (b)

Fig. 3. (a) Steel mold with induction heater on hydraulic press; (b) mold parts.

of cold production was performed on an XRD-6000 X-ray diffractometer (*Shimadzu*, Kyoto, Japan) with CuKα radiation in the range of $10° \le 2\theta \le 70°$ at a step of $2\theta = 0.02°$. The samples diffraction patterns were compared with the data of PDF-2 database [20].

RESULTS AND DISCUSSION

A micrograph of the initial $(MnFeCoNiCu)_3O_4$ powder after synthesis is shown in Fig. 4. As typical for powders obtained by low-temperature self-propagating synthesis (bulk combustion), the powder consists of large particles of porous agglomerates. An analysis of the granulometric composition (Table 1) confirmed the presence of predominantly large agglomerates with a modal diameter d_M = 45.9 μm. After ultrasonic treatment, the average particle size decreased by about half, that is, the use of ultrasonics led to the destruction of a considerable amount of large agglomerates and aggregates. The pycnometric density of the powder as measured by the Archimedes method was 5.14 g/cm^3.

As a result of a series of CSP experiments of $(MnFeCoNiCu)_3O_4$ powder it was found that the relative density of samples ≥0.70 can only be achieved using distilled water or aqueous solutions of CH_3COONH_4 and NaOH (Table 2). When applying a compression-molding pressure of 315 MPa, a holding time of 30 min, a heating time of 20 min, and an additive concentration of 0.1 wt %, the highest relative density of the samples was consistently achieved at 300°C. The samples had sufficient transport strength for extraction from the mold, measurement of relative density by the Archimedes method, and subsequent measurements of electrical and magnetic properties. (The results of studies on the physical properties of samples of high-entropy ceramics will be presented in a separate publication.) It is possible that the process temperature could be reduced by increasing the concentration of effective activating additives (CH_3COONH_4 and NaOH) while maintaining relative density values above 0.70. However, under such experimental conditions, an increase in the CSP temperature is impossible due to the strong adhesion of the sample to punches at 350°C [19].

The densest CSP (Fig. 5) obtained using water and aqueous solutions of CH_3COONH_4 and NaOH, were studied by SEM and X-ray diffraction analysis. An analysis of the microstructures of samples (Fig. 6) obtained at different compositions of the liquid phase and identical CSP conditions indicates a noticeable effect of activating additives CH_3COONH_4 and NaOH. When using

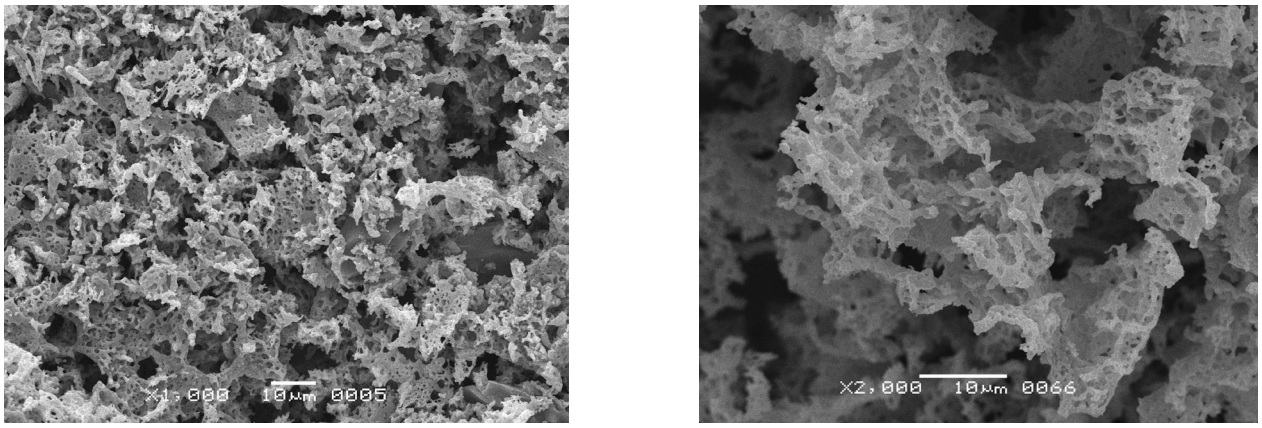

Fig. 4. SEM image of the $(MnFeCoNiCu)_3O_4$ powder.

Table 1. Results of the granulometric composition measurement for $(MnFeCoNiCu)_3O_4$ powder

No.	Conditions	d_M, μm	d_{10}, μm	d_{50}, μm	d_{90}, μm	S_{sp}, * cm^2/cm^3
1	Without ultrasonic treatment	45.9	8.9	32.0	73.8	3466
2	After ultrasonic treatment	20.4	6.0	18.1	36.4	5145

* S_{sp} is the specific surface area.

Table 2. Effect of activating additives on the relative density of cold-sintered samples

Activating additive	Temperature, °C	Cold sintering modes*	Relative density
H_2O	250	P = 315 MPa t = 30 min	0.69
	300		0.71
CH_3COONH_4	250		0.68
	300		0.70
CH_3COOH	250		0.65
	300		0.67
NH_4Cl	250		0.64
	300		0.65
$KF·2H_2$	250		0.54
	300		0.55
LiF	250		0.60
	300		0.59
NaF	250		0.63
	300		0.64
NaOH	250		0.70
	300		0.71

* P is the compression-molding pressure; t is the holding time.

distilled water, there is a change in the morphology of the initial powder particles, the formation of grains, their compaction, and a slight increase in size (Fig. 6a). It can be concluded that the presence of 20 wt % of distilled water and a mechanical pressure of 315 MPa are sufficient to initiate the CSP of a powder of the composition $(MnFeCoNiCu)_3O_4$ at a temperature of 300°C for 30 min. When adding 0.1 wt % CH_3COONH_4 (Fig. 6b) and NaOH (Fig. 6c), a pronounced grain growth is observed upon reaching close values of relative density (0.70 and 0.71, respectively). The CSP proceeds more intensively in an aqueous medium containing CH_3COONH_4 and NaOH. In the case of a powder of the composition $(MnFeCoNiCu)_3O_4$ these activating additives initiate the dissolution of the powder particles surface and/or increase

Fig. 5. Cold-sintered ceramic sample from $(MnFeCoNiCu)_3O_4$ powder, relative density 0.71 (temperature 300°C, 0.1 wt % of NaOH).

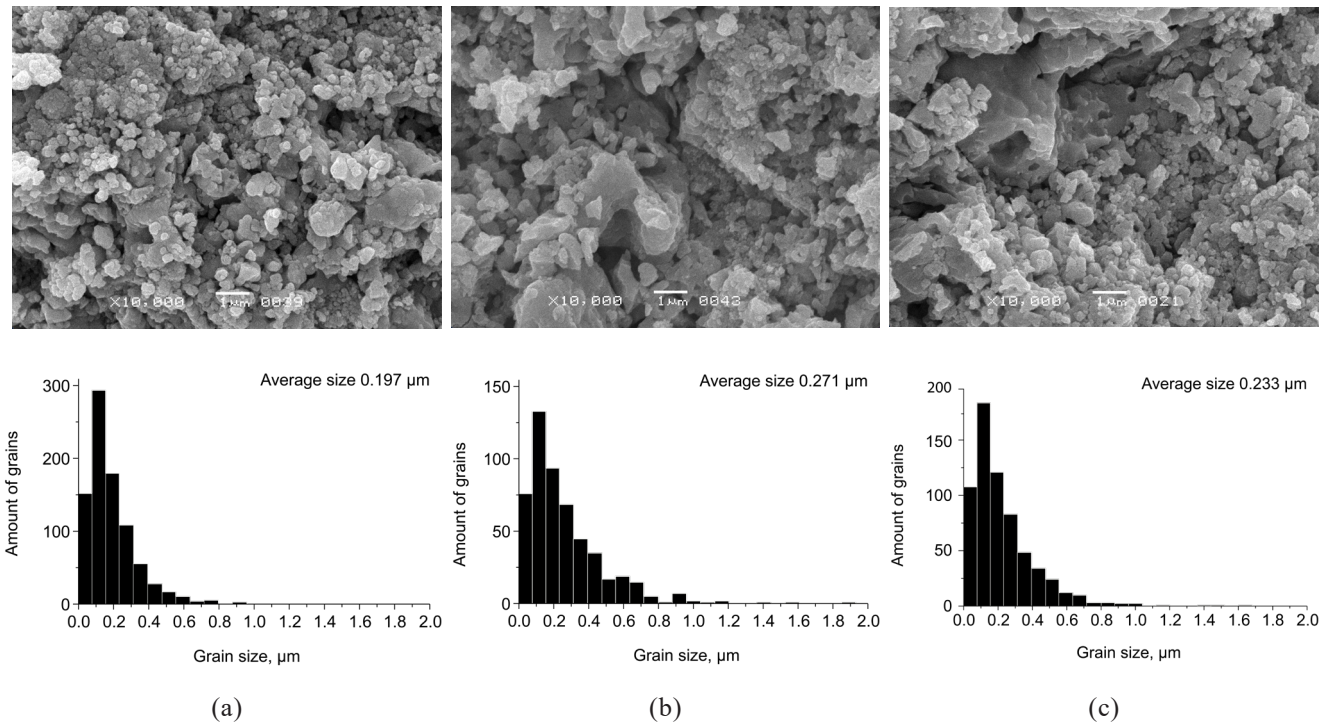

Fig. 6. Microstructure and particle size distribution histogram of cold-sintered $(MnFeCoNiCu)_3O_4$ ceramic samples obtained at different compositions of the liquid phase: (a) H_2O; (b) 0.1 wt % CH_3COONH_4; (c) 0.1 wt % NaOH. Temperature 300 °C, compression-molding pressure 315 MPa, dwell 30 min.

the number of defects in the surface layer of the particles of the powder material and, as a result, increase the solid-phase mobility of its crystal structure. For a detailed study of the effect of CH_3COONH_4 and NaOH on the microstructure and properties of high-entropy cold-sintering ceramics of the composition $(MnFeCoNiCu)_3O_4$, further studies of grain size distribution using SEM image analysis, characterization of the electrical and magnetic properties of samples depending on the activating additive concentration and process modes are planned.

Figure 7 shows the results of X-ray diffraction analysis of the phase composition of the initial powder (Fig. 7a) and cold sintering samples (Figs. 7b–7d). All diffraction patterns have identical reflection patterns corresponding to the phase with the spinel structure and additional reflections indicating the presence of a second phase with the rock salt structure. The presence of two phases distinguishes the high-entropy oxide ceramic $(MnFeCoNiCu)_3O_4$ studied in this work from the material of similar chemical composition described in [21], but having only one phase with a spinel structure. This fact is of considerable interest, since the properties of one- and two-phase high-entropy ceramics $(MnFeCoNiCu)_3O_4$ can vary significantly. In general, it can be stated that

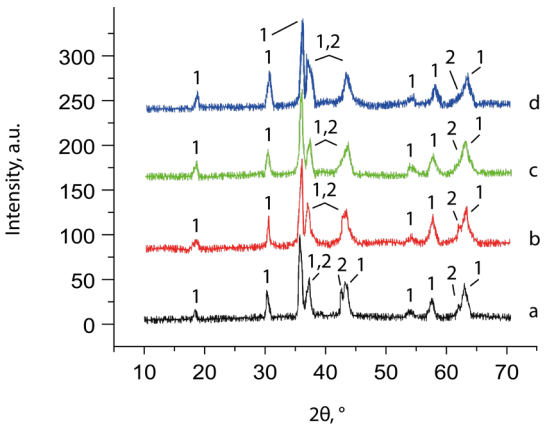

Fig. 7. XRD patterns of:
(a) initial powder $(MnFeCoNiCu)_3O_4$;
(b) cold-sintered sample, 0.1 wt % of NaOH;
(c) cold-sintered sample, 0.1 wt % of CH_3COONH_4;
(d) cold-sintered sample, H_2O.
Phase types indicated: 1—spinel; 2—rock salt. Temperature 300°C, compression-molding pressure 315 MPa, dwell 30 min.

the CSP of $(MnFeCoNiCu)_3O_4$ powder at 300°C using an aqueous medium with the addition of 0.1 wt % of CH_3COONH_4 and NaOH does not lead to a change in the initial powder phase composition. This indicates that the high-entropy structure has been preserved.

CONCLUSIONS

For the first time, the influence of the activating additive type on the relative density of samples of high-entropy ceramics $(MnFeCoNiCu)_3O_4$ obtained by the CSP is shown experimentally. Ceramic samples with a relative density of 0.70–0.71 were obtained using 20 wt % of distilled water or an aqueous solution of 0.1 wt % of CH_3COONH_4 or NaOH as a liquid medium. Samples of high-entropy ceramic material were obtained at a temperature of 300°C, a holding time of 30 min, and a compression-molding pressure of 315 MPa. The microstructures of the samples have pronounced differences: 20 wt % of distilled water does not lead to a pronounced growth of grains, only their compaction to 0.71 relative density is observed. When adding 0.1 wt % of CH_3COONH_4 and NaOH, a noticeable grain growth is observed upon reaching close values of relative density (0.70 and 0.71, respectively). For a more detailed study of this effect, further studies on the grain size distribution and physical properties of samples depending on the activating additive concentration and process modes are necessary. X-ray diffraction analysis showed that the CSP of $(MnFeCoNiCu)_3O_4$ powder at a temperature of 300°C and using an aqueous medium with the addition of 0.1 wt % of CH_3COONH_4 and NaOH does not lead to a change in the phase composition of the initial powder, which indicates the preservation of the high entropy structure.

Acknowledgments

The study was supported by the Ministry of Science and Higher Education of the Russian Federation, Agreement No. 075-15-2021-974 of September 28, 2021. The applied research was conducted on the topic of "Development of technological methods for reducing the sintering temperature of high-entropy ceramic materials based on transition metal oxides." The work was carried out with the use of equipment of the Joint Educational and Scientific Center for Collective Use at the MIREA – Russian Technological University and the Center for Collective Use "High-Tech Technologies of Mechanical Engineering" at the Moscow Polytechnic University.

Also, the work was supported by the Science Committee of the Ministry of Education, Science, Culture and Sports of the Republic of Armenia, the research project No. 20TTWS-2F040.

Authors' contributions

A.V. Smirnov – research conceptualization and writing the text of the article;

Yu.D. Ivakin – research conceptualization, selection of activating additives, microstructure analysis, and editing the text of the article;

M.V. Kornyushin – conducting research and data curation;

A.A. Kholodkova – analysis of X-ray diffractograms and editing the text of the article;

A.A. Vasin – visualization and editing the text of the article;

S. Aydinyan – initial powder synthesis and editing the text of the article;

A.V. Kirakosyan – initial powder synthesis and editing the text of the article.

The authors declare no conflict of interest.

REFERENCES

1. Yeh J.-W., Chen S.-K., Lin S.-J., Gan J.-Y., Chin T.-S., Shun T.-T., *et al*. Nanostructured High-Entropy Alloys with Multiple Principal Elements: Novel Alloy Design Concepts and Outcomes. *Adv. Eng. Mater.* 2004;6(5):299–303. https://doi.org/10.1002/adem.200300567

2. George E.P., Raabe D., Ritchie R.O. High-entropy alloys. *Nat. Rev. Mater*. 2019;4(8):515–34. https://doi.org/10.1038/s41578-019-0121-4

3. Oses C., Toher C., Curtarolo S. High-entropy ceramics. *Nat. Rev. Mater*. 2020;5(4):295–309. https://doi.org/10.1038/s41578-019-0170-8

4. Dąbrowa J., Stygar M., Mikuła A., Knapik A., Mroczka K., Tejchman W., *et al*. Synthesis and microstructure of the $(Co,Cr,Fe,Mn,Ni)_3O_4$ high entropy oxide characterized by spinel structure. *Mater. Lett*. 2018;216:32–6. https://doi.org/10.1016/j.matlet.2017.12.148

5. Mao A., Quan F., Xiang H.-Z., Zhang Z.-G., Kuramoto K., Xia A.-L. Facile synthesis and ferrimagnetic property of spinel $(CoCrFeMnNi)_3O_4$ high-entropy oxide nanocrystalline powder. *J. Mol. Struct*. 2019;1194:11–18. https://doi.org/10.1016/j.molstruc.2019.05.073

6. Mao A., Xiang H.-Z., Zhang Z.-G., Kuramoto K., Zhang H., Jia Y. A new class of spinel high-entropy oxides with controllable magnetic properties. *J. Magn. Magn. Mater*. 2020;497:165884. https://doi.org/10.1016/j.jmmm.2019.165884

7. Witte R., Sarkar A., Kruk R., Eggert B., Brand R.A., Wende H., *et al*. High-entropy oxides: An emerging prospect for magnetic rare-earth transition metal perovskites. *Phys. Rev. Mater*. 201913;3(3):034406. https://doi.org/10.1103/PhysRevMaterials.3.034406

8. Jimenez-Segura M.P., Takayama T., Bérardan D., Hoser A., Reehuis M., Takagi H., *et al*. Long-range magnetic ordering in rocksalt-type high-entropy oxides. *Appl. Phys. Lett*. 2019;114(12):122401. https://doi.org/10.1063/1.5091787

9. Dai S., Li M., Wang X., Zhu H., Zhao Y., Wu Z. Fabrication and magnetic property of novel $(Co,Zn,Fe,Mn,Ni)_3O_4$ high-entropy spinel oxide. *J. Magn. Magn. Mater*. 2021;536:168123. https://doi.org/10.1016/j.jmmm.2021.168123

10. Bordia R.K., Kang S.L., Olevsky E.A. Current understanding and future research directions at the onset of the next century of sintering science and technology. *J. Am. Ceram. Soc*. 2017;100(6):2314–2352. https://doi.org/10.1111/jace.14919

11. Guo J., Floyd R., Lowum S., Maria J.-P., Herisson de Beauvoir T., Seo J.-H., Randall C.A. Cold Sintering: Progress, Challenges, and Future Opportunities. *Annu. Rev. Mater. Res*. 2019;49(1):275–295. https://doi.org/10.1146/annurev-matsci-070218-010041

12. Maria J.-P., Kang X., Floyd R.D., Dickey E.C., Guo H., Guo J., *et al*. Cold sintering: Current status and prospects. *J. Mater. Res*. 2017;32(17):3205–3218. https://doi.org/10.1557/jmr.2017.262

13. Gonzalez-Julian J., Neuhaus K., Bernemann M., Pereira da Silva J., Laptev A., Bram M., *et al*. Unveiling the mechanisms of cold sintering of ZnO at 250 °C by varying applied stress and characterizing grain boundaries by Kelvin Probe Force Microscopy. *Acta Mater*. 2018;144(1):116–128. https://doi.org/10.1016/j.actamat.2017.10.055

14. Galotta A., Sglavo V.M. The cold sintering process: A review on processing features, densification mechanisms and perspectives. *J. Eur. Ceram. Soc*. 2021;41(16):1–17. https://doi.org/10.1016/j.jeurceramsoc.2021.09.024

15. Ivakin Y., Smirnov A., Kholodkova A., Vasin A., Kormilicin M., Kornyushin M., *et al*. Comparative Study of Cold Sintering Process and Autoclave Thermo-Vapor Treatment on a ZnO Sample. *Crystals*. 2021;11(1):71. https://doi.org/10.3390/cryst11010071

16. Ivakin Yu.D., Smirnov A.V., Kormilitsin M.N., Kholodkova A.A., Vasin A.A., Kornyushin M.V., Tarasovskii V.P., Rybal'chenko V.V. Effect of Mechanical Pressure on the Recrystallization of Zinc Oxide in a Water Fluid Medium under Cold Sintering. *Russ. J. Phys. Chem. B.* 2021;15(8):1228–1250. https://doi.org/10.1134/S1990793121080054

17. Ivakin Y.D., Smirnov A.V., Kurmysheva A.Yu., Kharlanov A.N., Solís Pinargote N.W., Smirnov A., *et al*. The Role of the Activator Additives Introduction Method in the Cold Sintering Process of ZnO Ceramics: CSP/SPS Approach. *Materials.* 2021;14(21):6680. https://doi.org/10.3390/ma14216680

18. Nakajima T., Žemva B., Tressaud A. *Advanced Inorganic Fluorides: Synthesis, Characterization and Applications*. Elsevier; 2000. 701 p. https://doi.org/10.1016/B978-0-444-72002-3.X5000-5

19. Smirnov A.V., *et al*. The Cold Sintering Process of High-Entropy Ceramics $(MnFeCoNiCu)_3O_4$. *Int. J. Mech. Eng*. 2021;6(3):1–6.

20. Gates-Rector S., Blanton T. The Powder Diffraction File: A Quality Materials Characterization Database. *Powder Diffr*. 2019;34(4):352–360. https://doi.org/10.1017/S0885715619000812

21. Wang D., Liu Z., Du S., Zhang Y., Li H., Xiao Z., *et al*. Low-temperature synthesis of small-sized high-entropy oxides for water oxidation. *J. Mater. Chem. A.* 2019;7(42):24211–24216. https://doi.org/10.1039/C9TA08740K

About the authors:

Andrey V. Smirnov, Cand. Sci. (Eng.), Head of the Department of Advanced Materials Technologies of the Mobile Solutions Engineering Center, MIREA – Russian Technological University (78, Vernadskogo pr., Moscow, 119454, Russia). E-mail: smirnov_av@mirea.ru. ResearcherID J-2763-2017, Scopus Author ID 56970389000, RSCI SPIN-code 2919-9250, https://orcid.org/0000-0002-4415-5747

Yuri D. Ivakin, Cand. Sci. (Chem.), Senior Researcher, Department of Physical Chemistry, Faculty of Chemistry, Lomonosov Moscow State University (1-3, Kolmogorova ul., Moscow, 119234, Russia). E-mail: yu.ivakin@mail.ru. ResearcherID N-9483-2013, Scopus Author ID 6603058433, RSCI SPIN-code 7337-4173, https://orcid.org/0000-0002-8416-3071

Maxim V. Kornyushin, Engineer, Laboratory of Ceramic and Composite Materials of the Mobile Solutions Engineering Center, MIREA – Russian Technological University (78, Vernadskogo pr., Moscow, 119454, Russia). E-mail: kornyushin@mirea.ru. Scopus Author ID 57219230569, RSCI SPIN-code 7995-3408, https://orcid.org/0000-0001-6104-7716

Anastasia A. Kholodkova, Cand. Sci. (Chem.), Junior Researcher, Department of Physical Chemistry, Faculty of Chemistry, Lomonosov Moscow State University (1-3, Kolmogorova ul., Moscow, 119234, Russia). E-mail: anakholo@gmail.com. ResearcherID M-2169-2016, Scopus Author ID 56530861400, RSCI SPIN-code 7256-7784, https://orcid.org/0000-0002-9627-2355

Alexander A. Vasin, Cand. Sci. (Eng.), Leading Researcher, Laboratory of Ceramic and Composite Materials of the Engineering Center for Mobile Solutions, MIREA – Russian Technological University (78, Vernadskogo pr., Moscow, 119454, Russia). E-mail: alexandrvasin123@gmail.com. ResearcherID K-3214-2015, Scopus Author ID 57211840246, RSCI SPIN-code 3864-9132, https://orcid.org/0000-0002-9501-2316

Sofia Aydinyan, Cand. Sci. (Chem.), Senior Researcher, A.B. Nalbandyan Institute of Chemical Physics (5/2, P. Sevak ul., Yerevan, 0014, Armenia). E-mail: sofiyaaydinyan25@gmail.com. Scopus Author ID 24479551800, https://orcid.org/0000-0001-6530-6308

Hasmik V. Kirakosyan, Cand. Sci. (Chem.), Junior Researcher, A.B. Nalbandyan Institute of Chemical Physics (5/2, P. Sevak ul., Yerevan, 0014, Armenia). E-mail: hasmik-kirakosyan@list.ru. Scopus Author ID 56925595700, https://orcid.org/0000-0003-1103-7952

Об авторах:

Смирнов Андрей Владимирович, к.т.н., заведующий отделением технологий перспективных материалов Инжинирингового центра мобильных решений, ФГБОУ ВО «МИРЭА – Российский технологический университет» (119454, Россия, Москва, пр-т Вернадского, д. 78). E-mail: smirnov_av@mirea.ru. ResearcherID J-2763-2017, Scopus Author ID 56970389000, SPIN-код РИНЦ 2919-9250, https://orcid.org/0000-0002-4415-5747

Ивакин Юрий Дмитриевич, к.х.н., старший научный сотрудник кафедры физической химии, Химический факультет, ФГБОУ ВО «Московский государственный университет им. М.В. Ломоносова» (119234, Россия, Москва, ул. Колмогорова, 1, стр. 3). E-mail: yu.ivakin@mail.ru. ResearcherID N-9483-2013, Scopus Author ID 6603058433, SPIN-код РИНЦ 7337-4173, https://orcid.org/0000-0002-8416-3071

Корнюшин Максим Витальевич, инженер лаборатории керамических и композиционных материалов Инжинирингового центра мобильных решений, ФГБОУ ВО «МИРЭА – Российский технологический университет» (119454, Россия, Москва, пр-т Вернадского, д. 78). E-mail: kornyushin@mirea.ru. Scopus Author ID 57219230569, SPIN-код РИНЦ 7995-3408, https://orcid.org/0000-0001-6104-7716

Холодкова Анастасия Андреевна, к.х.н., младший научный сотрудник кафедры физической химии, Химический факультет, ФГБОУ ВО «Московский государственный университет им. М.В. Ломоносова» (119234, Россия, Москва, ул. Колмогорова, 1, стр. 3). E-mail: anakholo@gmail.com. ResearcherID M-2169-2016, Scopus Author ID 56530861400, SPIN-код РИНЦ 7256-7784, https://orcid.org/0000-0002-9627-2355

Васин Александр Александрович, к.т.н., ведущий научный сотрудник лаборатории керамических и композиционных материалов Инжинирингового центра мобильных решений, ФГБОУ ВО «МИРЭА – Российский технологический университет» (119454, Россия, Москва, пр-т Вернадского, д. 78). E-mail: alexandrvasin123@gmail.com. Researcher ID K-3214-2015, Scopus Author ID 57211840246, SPIN-код РИНЦ 3864-9132, https://orcid.org/0000-0002-9501-2316

София Айдинян, к.х.н., старший научный сотрудник, Институт химической физики им. А.Б. Налбандяна (0014, Армения, Ереван, ул. П. Севака, д. 5/2). E-mail: sofiyaaydinyan25@gmail.com. Scopus Author ID 24479551800, https://orcid.org/0000-0001-6530-6308

Асмик В. Киракосян, к.х.н., младший научный сотрудник, Институт химической физики им. А.Б. Налбандяна (0014, Армения, Ереван, ул. П. Севака, д. 5/2). E-mail: hasmik-kirakosyan@list.ru. Scopus Author ID 56925595700, https://orcid.org/0000-0003-1103-7952

The article was submitted: April 19, 2022; approved after reviewing: July 08, 2022; accepted for publication: September 16, 2022.

Translated from Russian into English by M. Povorin
Edited for English language and spelling by Thomas Beavitt